

Cubic Cu_xZrO_{100-x} as an efficient and selective catalyst for the oxidation of aromatics active methyl, alcohol, and amine groups



Balasaheb D. Bankar^{a,b}, Jacky H. Advani^{a,b}, Ankush V. Biradar^{a,b,*}

^aInorganic Materials and Catalysis Division, CSIR-Central Salt and Marine Chemicals Research Institute (CSIR-CSMCRI), G. B. Marg, Bhavnagar 364002, Gujarat, India

^bAcademy of Scientific and Innovative Research (AcSIR), Ghaziabad 201002, Uttar Pradesh, India

ARTICLE INFO

Article history:

Received 30 November 2020

Accepted 20 February 2021

Available online 27 February 2021

Keyword:

Mixed metal oxide
Heterogeneous catalyst
Hydrothermal synthesis
Oxidation
Functional groups

ABSTRACT

The local structure of a supported active metal plays a vital role in determining the desired product's selectivity in heterogeneous catalysis. Herein, we have developed a simple protocol for the synthesis of Cu doped on cubic ZrO₂ mixed metal oxide catalysts and used it for the selective oxidation of various functional groups. The catalyst was synthesized by varying the wt.% of Cu (1–20%) on ZrO₂ by co-precipitation, followed by hydrothermal treatment. The X-ray diffraction pattern of the catalysts confirmed the formation of the cubic phase of ZrO₂, and the growth of CuO occurred along the (1 1 1) plane. The microscopy analysis revealed the uniform distribution of Cu on the ZrO₂ surface, while XPS analysis confirmed the presence of copper in the +2 oxidation state. The synthesized catalyst with 2 wt% loading of Cu on ZrO₂ showed excellent liquid-phase oxidation properties and gave good to best conversion of active methyl groups, alcohols, and amines with high selectivities to corresponding ketones, aldehydes, and amides, respectively, under milder reaction conditions. Furthermore, the synthesized catalyst showed a broader substrate scope for the various substituted active methyl groups, alcohols, and amines with good conversion and selectivity.

© 2021 Elsevier Ltd. All rights reserved.

1. Introduction

Mixed metal oxides (MMOs) are widely used in many areas of science, including chemistry, physics, and material science. Mainly, MMOs have been found to be potential candidates for catalysis, owing to their tunable physical and chemical properties (acidic, basic) and morphological changes [1]. However, most of the reported MMOs are in bulk, and the exact nature of the active species involved is still a widely studied subject [2,3]. Thus, understanding the catalytic activity associated with such a complex system is extensively carried out by different synthetic methods [4]. Notably, copper-containing materials have received attention because of their oxidative properties and lower cost compared to noble metal-based catalysts. The key feature of copper metals involves its interaction with other metals, both geometrically as well as electronically, and the variable oxidation states [5]. Hence, it has been widely used in various catalytic reactions. For instance, the halogenation of aromatic compounds was carried by a heterogeneous Cu-containing CuMn spinel oxide catalyst for the regioselective halogenation of phenol and *N*-hetero aromatic compounds [6]. In another report, Xie *et al.* report the mixed metal oxide

hierarchical flower-like Al₂O₃@CoCuAl microspheres catalyst for selective ethylbenzene oxidation with 92.8% conversion and 89.4% selectivity for acetophenone [7]. Shukla *et al.* utilized a surfactant-assisted hydrothermal method to prepare a CuCeO₂ catalyst to oxidize aromatic amines to azoxy compounds using H₂O₂ [8]. Sadjadi *et al.* synthesized a Cu/MgO catalyst by a co-precipitation method and used it for vapor-phase hydrogenation of furfural to furfural alcohol with excellent conversion (89%) and selectivity (97%) in 240 min [9]. Petitjean *et al.* reported copper doped porous metal oxide catalyst synthesized by a co-precipitation method for hydrogenation of alkenes and carbonyl groups [10].

Zirconia-supported Cu-containing catalysts have been intensively developed to improve the catalytic performance and selectivity for the reduction of CO₂ and other organic compounds. In particular, Tada *et al.* designed an active interfacial site with Cu loaded on an amorphous ZrO₂ bimetallic catalyst for the reduction of CO₂ to methanol at high temperature (230 °C) and pressure (10 bar) [11–13]. Zhong *et al.* used a similar type of material for methanol synthesis from CO₂ under milder conditions at 240 °C, and pressure of 3.0 MPa, a CO₂ conversion of 9.9% with 45% selectivity and 4.5% yield towards methanol at 3600 h⁻¹ GHSV was observed [14].

These literature reports indicate that, in heterogeneous catalysis, support plays an important role in achieving high activity

* Corresponding author.

E-mail address: ankush@csmcri.res.in (A.V. Biradar).

and selectivity by stabilizing the active metal intermediate species, preventing the sintering of active metals, and providing an electrophilic and nucleophilic environment [15,16]. Among the different supports utilized, ZrO₂ finds a special place in catalysis owing to its amphoteric nature, thermal stability, variable phases, and tuneable surface area. The high thermal stability of cubic ZrO₂ (2400 °C) as compared to its analogues, i.e., monoclinic (1100 °C) and tetragonal (1400 °C) [17] and the presence of both acidic and basic sites on the surface, and it makes an excellent candidate for redox type of catalysis [18]. Furthermore, zirconia was stabilized into the cubic phase using copper and nickel oxide and used for light alkane oxidation [19,20]. Considering these points, herein, we have developed a facile synthetic method for the synthesis of active Cu-containing Zr-supported metal oxide catalysts by a co-precipitation-hydrothermal method at milder temperatures. The catalyst is active towards the liquid-phase oxidation of alkanes, alcohols, and amines under mild reaction conditions, which might result from the structural aspect arising from the synthetic procedure.

2. Experimental

See Supporting information for materials and methods (SI, S1-S2).

2.1. Synthesis of Cu_xZrO_{100-x}

The Cu_xZrO_{100-x} catalyst was synthesized by loading different wt.% of copper ($x = 1-20\%$) through a combination of the co-precipitation-hydrothermal method. In a typical synthesis, 10 g of ZrO(NO₃)₂·xH₂O was added to 50 mL of distilled water and stirred for 30 min at room temperature until complete dissolution. Then, the required amount of Cu(NO₃)₂·3H₂O was added to this solution. After the solution became homogeneous, 5.5 mL ammonia solution (25%) was added dropwise as a co-precipitating agent, maintaining a constant pH 9. Further, the reaction mixture was aged by stirring for 20 h at room temperature and transferred to a 100 mL stainless steel hydrothermal reactor and kept in a muffle furnace at 180 °C for 3.5 h. After cooling the reactor to room temperature, the solid was collected by simple filtration and washed several times with deionized water until the filtrate showed neutral pH and then finally washed with 10 mL methanol. The obtained solid was dried in an oven at 70 °C for overnight and calcined in a muffle furnace at 500 °C at the heating rate of 5 °C/min for 5 h.

2.2. Synthesis of ZrO₂

The synthesis of pristine ZrO₂ was also carried out using a similar procedure as above without the addition of copper salt.

2.3. Catalytic activity

The liquid-phase oxidation reaction was performed in a two-necked dry 25 mL round-bottom flask. Typically, 1 mmol of the substrate, 3 mmol aq. TBHP, 15 mg of freshly prepared Cu_xZrO_{100-x} catalyst, 2 mL acetonitrile as a solvent, and chlorobenzene as an internal standard were mixed. The reaction mixture was heated to the desired temperature using a temperature-controlled oil bath. The progress of the reaction was monitored by withdrawing reaction aliquots, which were analyzed by gas chromatography (Agilent GC-7890B) and GC-MS (Shimadzu, QP-2010, Japan) with HP-5 column (5% diphenyl and 95% dimethyl polysiloxane capillary column). The catalyst was collected by filtration, washed twice with acetone (2 × 10 mL), dried in an oven at 100 °C for 5 h, and reused for the next cycle (See in S11 Table S4).

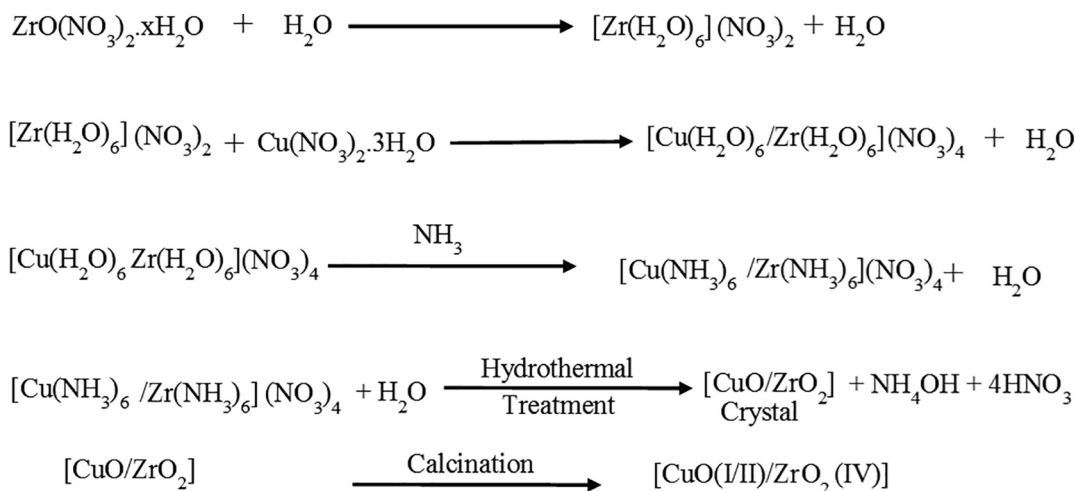
3. Results and discussion

For the synthesis of Cu_xZrO_{100-x} mixed metal oxide catalyst, a combination of co-precipitation followed by the hydrothermal method was used. A co-precipitation method aids in exchanging ligands giving metal complexes with catalytically active phases, while hydrothermal processes yield crystalline metal oxides under aqueous solutions, temperature, and autogenous pressure conditions. Hydrothermal synthesis is usually carried out below 300 °C. Water in supercritical conditions favours particle growth by increasing reaction rate and supersaturation based on the nucleation theory [21]. The metal salt-containing aqueous solution changes the reaction equilibrium, which results in the formation of metal hydroxide or metal oxides. Scheme 1 shows the formation of hydrated zirconia from zirconium nitrate aqueous solution [22] followed by the addition of aqueous copper nitrate with stirring to yield a hydrated complex of both metals. The addition of aqueous NH₃ solution act as a co-precipitating agent by dissociating hydroxyl complex (NH₃ being a strong ligand) forming an ammonium complex, which is stabilized by dissociated nitrate groups. During the course of the reaction, it produces monomers, followed by nucleation and crystal growth, and then finally calcined at high temperature to remove impurities to produce a phase pure oxide [23]. The material was characterized using various physicochemical methods (see SI, S3).

The phase purity of the materials was confirmed by PXRD (Fig. 1A). The diffraction peaks at $2\theta = 30.5, 35.3, 50.7, 60.2, 62.9$ and 74.6° correspond to the crystal planes (111), (200), (220), (311), (222), and (400) of cubic ZrO₂ support (JCPDS No. 00-027-0997). However, the diffraction peaks of Cu or CuO were not observed in the case of 1–5 wt% Cu on ZrO₂, maybe due to the lower wt.% of Cu, non-crystalline nature of Cu/CuO or may be due to Cu been repressed inside the zirconia support [24]. However, a shift in the diffraction peaks between the pure ZrO₂ and the Cu doped ZrO₂ could be observed, which may be attributed to the effect of copper loading in the ZrO₂ samples. The average crystallite particle size of the Cu_xZrO_{100-x} catalyst calculated from the (111) plane using the Debye-Scherrer equation and was found to be 8.60 nm (See SI, S4). The XRD profile of 20 wt% CuZrO₂ showed the presence of the peaks originating from the monoclinic CuO planes (200), (−200), (200), (202), (−113), (−311), (220) and (311) along with the ZrO₂ planes (See Fig. 1B or SI, S4). Thus, monoclinic CuO (JCPDS 04-005-4712) was loaded on ZrO₂ lattice.

FESEM analysis of the ZrO₂ support (Fig. 2a) as well as 2 wt% CuZrO₂ (Fig. 2b), both showed an irregular morphology. The uniform distribution of the elements was confirmed by elemental mapping of the catalyst, as shown in Fig. 2(c-f). HRTEM analysis confirmed the loading of copper onto the ZrO₂ support (Fig. 2g). The average particle size of 2 wt% CuZrO₂ catalyst was 5.3 nm (See SI, S6 fig.3.4). The fringes relating to the support, as well as CuO (111) and (200) phases, can be seen in (Fig. 2g₍₁₋₄₎). The d-spacing of the ZrO₂ support, as well as CuO, matches well with the JCPDS data. The CuO fringes from the (111) plane having a d-spacing of 0.232 nm can be seen in Fig. 2g₃. The SAED pattern of the 2 wt% CuZrO₂ (Fig. 2h) showed the presence of (220) and (422) facets of cubic ZrO₂ and (400) facets of Cu, supported in cubic zirconia phases (JCPDS file No. 00-004-0836). The FESEM and TEM analysis of other samples are given in SI, S6 Fig. S3.

The BET surface area and pore size of the series of Cu_xZrO_{100-x} catalysts measured by N₂ gas adsorption and desorption are tabulated in Table 1 (See SI, S7 Fig. S4). The surface area of pure ZrO₂ was 131.5 m²/g with a pore size of 132.6 Å. The increase in the loading wt.% of Cu from 1 to 5 wt% gave a decreasing trend in the surface area while pore size was found to increase. The ICP-OES analysis of the catalyst showed the presence of 1.95 wt% of



Scheme 1. Synthesis of $\text{Cu}_x\text{Zr}_{100-x}$ catalyst by a co-precipitation followed by hydrothermal method.

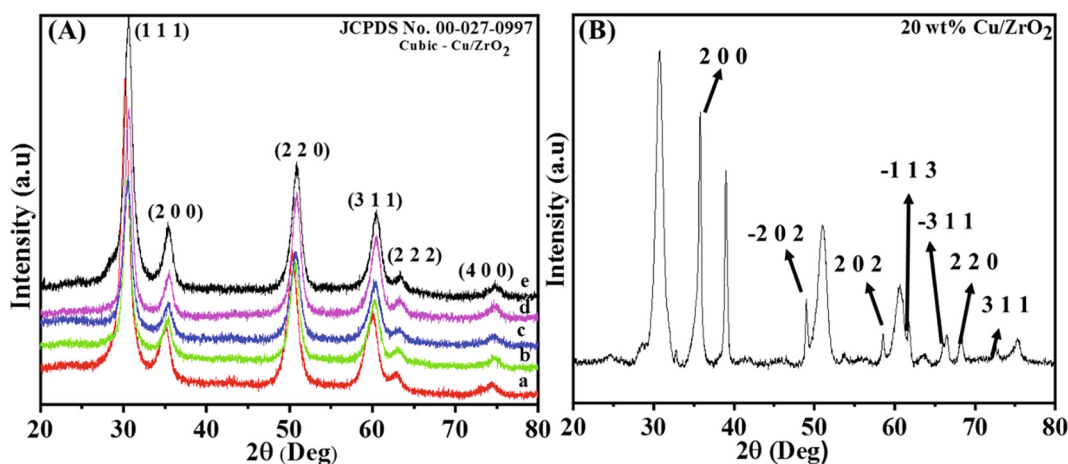


Fig. 1. XRD pattern of (A) (a) ZrO_2 ; (b) 1 wt% CuZrO_2 ; (c) 2 wt% CuZrO_2 ; (d) 3 wt% CuZrO_2 ; (e) 5 wt% CuZrO_2 . (B) 20 wt% CuZrO_2 .

the total copper in the sample. The cumulative quantity of the adsorbed H_2 gas, as confirmed by pulse TPR, was $4.334 \times 10^{-2} \text{ cm}^3/\text{g}$ at STP with metal dispersion of 0.244% and a metallic surface area $1.57 \text{ m}^2/\text{g}$. The copper dispersion was determined by pulse H_2 chemisorption. The cumulative quantity of the adsorbed H_2 gas was $8.635 \times 10^{-2} \text{ cm}^3/\text{g}$ at STP with metal dispersion of 0.2448% and a metallic surface area of $1.5778 \text{ m}^2/\text{g}$ and cubic crystal size of 355.2 nm.

The electronic state of the 2 wt% CuZrO_2 catalyst was confirmed by XPS studies (Fig. 3). The survey spectra of catalyst confirmed the presence of Cu, Zr, and O in the sample (Fig. 3A). The XPS spectra of Zr (Fig. 3B) showed the presence of a peak at binding energies of 182.5, 184.8, and 187.1 eV corresponding to Zr $3d_{5/2}$, $3d_{3/2}$, and $3d_{3/2}$, respectively [25]. The presence of the Cu $2p_{3/2}$ peak at the binding energies of 935.8 and 956 eV confirmed the presence of Cu^{+2} species in the material (Fig. 3C). The peak at a binding energy of 944.8 eV indicates the presence of a satellite peak of Cu^{2+} [26,27], confirming that Cu^{2+} is a significant species present in the material. Fig. 3D shows the XPS spectra of O 1s with three different peaks at 530.5, 533, and 535.5 eV, corresponding to the lattice oxygen species present in the material.

3.1. Catalytic reactions

The carbonyl functional groups are key intermediates in many organic molecules like perfume, pharmaceuticals, resins, and fla-

voring agents [28,29]. There are many synthetic methods reported for the synthesis of carbonyl compounds [30]. However, some or the other disadvantages are exist in these methods; hence there is always a need to search for alternative methods. The catalytic activity of the different synthesized $\text{Cu}_x\text{Zr}_{100-x}$ materials was evaluated for liquid-phase oxidation of various functional groups, including aromatic alkyl, alcohol, and amine.

For the optimization of the reaction conditions for the oxidation reaction, ethylbenzene was selected as a model substrate (Scheme 2). Initially, the oxidation of ethylbenzene in the absence of a catalyst did not show any conversion of ethylbenzene (Table 2). The use of pure ZrO_2 and 1 wt% CuZrO_2 as catalysts for this reaction in the absence of oxidant (TBHP), again gave no conversion of ethylbenzene (See Table 2, entries 2 and 3). This suggests that the reaction does not proceed in the absence of a catalyst and an oxidant. The use of 1 wt% CuZrO_2 as catalyst showed 55.2% conversion of ethylbenzene with 100% selectivity to acetophenone (See Table 2, entry 4). On increasing the copper loading to 2 wt%, an increase in the conversion of ethylbenzene to 98% with complete selectivity to acetophenone as the product was observed (See Table 2, entry 5). However, a further increase in the copper content did not improve the activity of the catalysts (Table 2, entries 5–8). When the oxidant to substrate molar ratio was 1, only 62.5% conversion of ethylbenzene was observed (Table 2, entry 9), while the reaction with oxidant to a molar ratio of 2 gave 89.5% conversion of ethylbenzene (Table 2, entry 10). Thus, we selected 2 wt% CuZrO_2

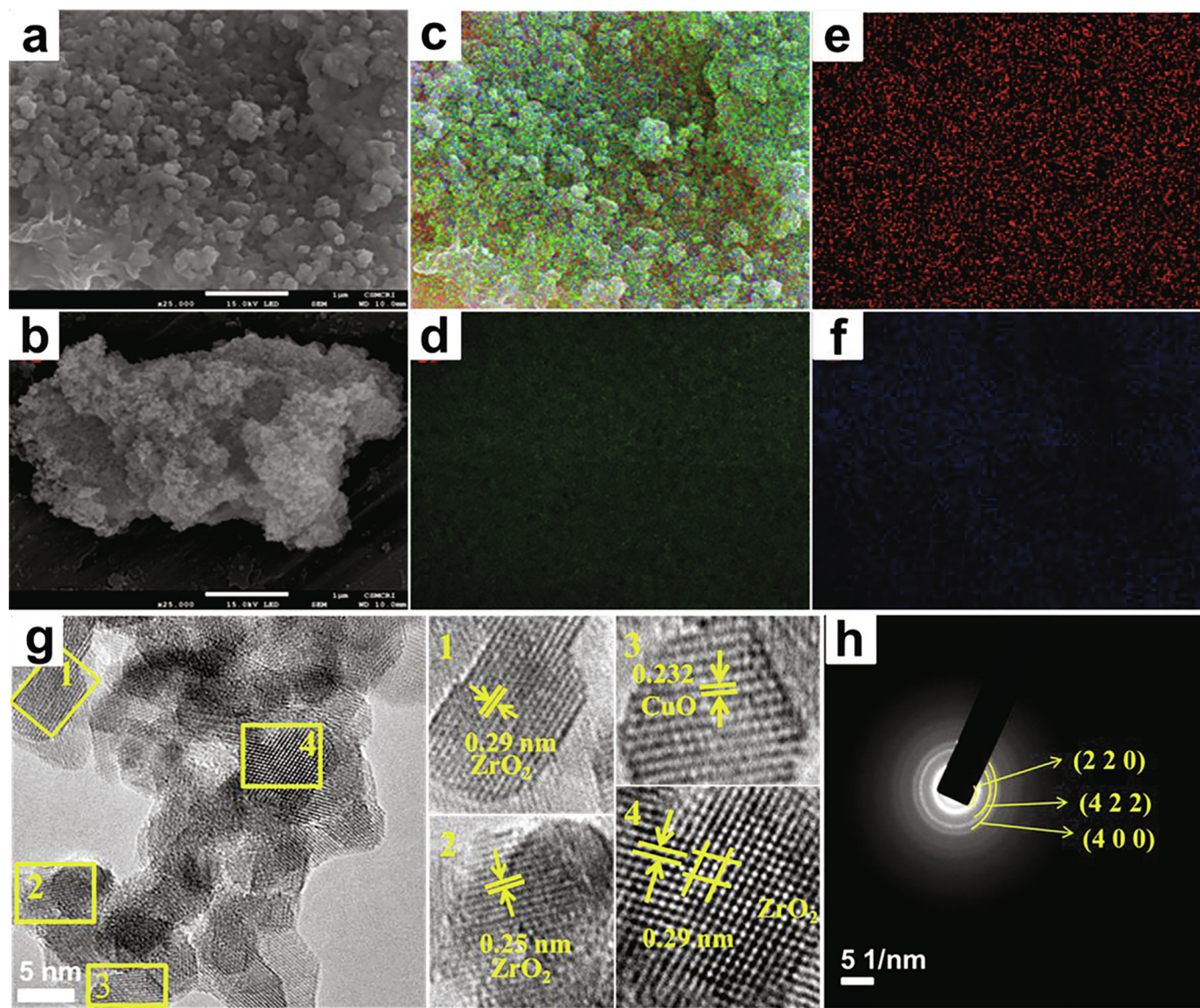


Fig. 2. SEM images of (a) ZrO_2 (scale 1 μm), (b) CuZrO_2 (scale 1 μm), elemental mapping of (c) Mix map of Cu, Zr and O, (d) Zr, (e) Cu; (f) O, (g) HRTEM images of 2 wt% CuZrO_2 showing different fringes in (g) 1. ZrO_2 , 2 ZrO_2 , 3. CuO , 4. ZrO_2 and (h) SAED pattern.

Table 1
Physical properties of synthesized catalysts.

Catalyst	Composition wt. %		BET surface area (m^2/g)	Pore Size in \AA
	Cu	ZrO_2		
ZrO_2	–	100	131	132
CuZrO_2	1	99	103	139
CuZrO_2	2	98	80	223
CuZrO_2	3	97	70	231
CuZrO_2	5	95	62	250

catalyst and oxidant to substrate molar ratio of 3 for further optimization of the reaction conditions.

Since the solvent plays a significant role in the dispersion of the substrate, catalyst as well as oxidant, the effect of the solvent on the oxidation of ethylbenzene was also studied (See SI, S8, Table S2). Often, these solvents are directly involved in the elementary step of the reaction. Most of the literature reported that polar aprotic solvents are favourable for oxidation reaction as compared to nonpolar solvents. However, to check a suitable solvent for this

reaction, different solvents were screened. When the reaction was carried out in toluene, only 25% ethylbenzene was converted to acetophenone (See SI, S8, Table S2, entry 1). When a polar protic solvent like *tert*-Butanol was used, the conversion of ethylbenzene increased to 44% (See SI, S8, Table S2, entry 2). Further, polar protic solvent like H_2O gave excellent conversion of ethylbenzene with 100% selectivity (See SI, S8, Table S2, entry 3). The highest conversion of ethylbenzene was achieved in the polar aprotic solvent. The use of DCM as an 87% solvent gave a conversion of ethylbenzene

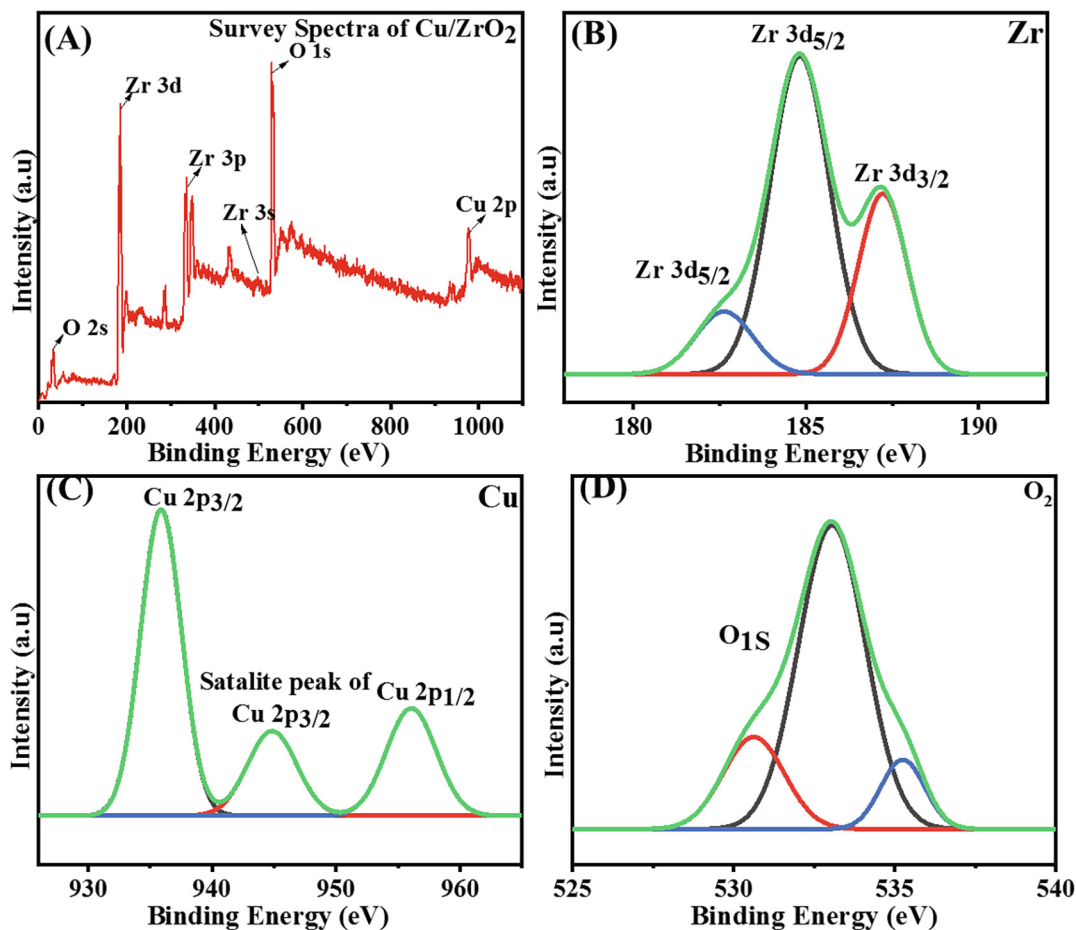
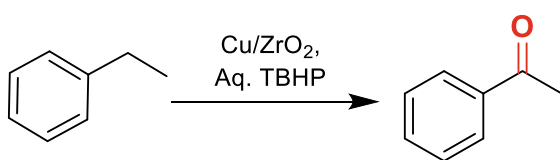


Fig. 3. XPS analysis of 2 wt% CuZrO₂ catalyst, (a) Survey spectra of the CuZrO₂, (b) Zr 3d, (c) Cu 2p, and (d) O 1s.



Scheme 2. Oxidation of ethylbenzene to acetophenone.

Table 2
Catalysts screening for the oxidation of ethylbenzene to acetophenone.^a

Entry	Catalyst	% Conversion	% Selectivity
1	Blank	0	0
2	Without Oxidant	0	0
3	ZrO ₂	0	0
4	1 wt% Cu _x ZrO _{100-x}	55.2	100
5	2 wt% Cu _x ZrO _{100-x}	98	100
6	3 wt% Cu _x ZrO _{100-x}	98.1	100
7	5 wt% Cu _x ZrO _{100-x}	98.3	100
8	20 wt% Cu _x ZrO _{100-x}	100	100
9 ^b	2 wt% Cu _x ZrO _{100-x}	62.5	100
10 ^c	2 wt% Cu _x ZrO _{100-x}	89.5	100

^aReaction Conditions: 2 mL Acetonitrile; Substrate: 1 mmol Ethylbenzene; Oxidant: 3 mmol Aq- TBHP; Catalyst: 15 mg, Cu/ZrO₂; Reaction temp.: 80 °C; Time: 18 h.; ^b Substrate: 1 mmol Ethylbenzene; Oxidant: 1 mmol Aq- TBHP; ^c Substrate: 1 mmol Ethylbenzene; Oxidant: 2 mmol Aq- TBHP.

(See SI, S8, Table S2, entry 4), while the use of the acetonitrile solvent gave 98% conversion with 100% selectivity (See SI, S8, Table S2, entry 5). Thus, we selected acetonitrile as the solvent

for further parametric study. The effect of reaction temperature on the oxidation of ethylbenzene was studied in the range of 60 to 80 °C (See SI, S9, Table S3). With an increase in the temperature of the reaction, the conversion of ethylbenzene increased from 44 to 95% with almost single product selectivity.

For the leaching studies, the catalyst was separated from the hot reaction mixture after 2 h (30% conversion), and the mixture was further allowed to react for 18 h. Only a 17% increase in the conversion was observed after the removal of the catalyst (See SI, S10, Fig. S5), which may be due to the remaining peroxy radical intermediate present in the mixture. ICP-OES analysis of the reaction mixture showed negligible copper leaching (0.0012%) (See SI, S10). The elemental mapping using the STEM analysis of the used catalyst confirmed the presence of the copper in the catalyst, thus confirming no leaching (See S10, Fig. S6). To probe the mechanistic route, we added 2 mmol of hydroxyl butylated toluene (HBT) as a quencher at the beginning of the reaction and allowed to react for 18 h. However, there was no conversion of ethylbenzene, which confirmed that the reaction occurred via a radical route. The catalytic performance of the synthesized catalyst for the oxidation of ethylbenzene was also compared to different reported heterogeneous catalysts with Cu supported catalysts and different metal complexes/oxide catalysts (See SI, S14). Also, the merit of metal-doped cubic ZrO₂ is well studied. Incorporation of the metal in the ZrO₂ bulk structure not only stabilizes the cubic (fluorite) metal oxide but also drastically increases the reactivity of the lattice oxygens, which can be used for the low-temperature oxidation reaction. It was also reported that CuO/ZrO₂ showed better oxidation activity than the other catalysts because of the easy reduction of

highly dispersed copper species on ZrO_2 [19,31]. As expected, our catalyst outperforms in the liquid phase oxidation reaction at low temperature.

Furthermore, the optimized reaction protocol was extended to various substrates using our best catalyst, i.e., 2 wt% $CuZrO_2$ catalyst and aq. TBHP as an oxidant. The oxidation of ethylbenzene using the $CuZrO_2$ catalyst gave 98% conversion with complete selectivity towards acetophenone (Table 2, entry 1).

When highly reactive diphenylmethane was used as a substrate, it was completely oxidized to give benzophenone as the sole product. The presence of phenyl ring on both sides of the active methyl group makes it more reactive, and thus, it easily oxidize (Table 3, entry 2). The effects of electron-withdrawing and donating groups on the substrate were also studied. The oxidation of 4-hydroxy ethylbenzene gave only 98% conversion (Table 3, entry 3), while that of 4-nitro ethylbenzene gave only 66% conversion (Table 3, entry 4). Furthermore, the oxidation of 4-chloro ethylbenzene gave 60% conversion with complete selectivity towards 4-chloro acetophenone. The oxidation of heterocyclic molecule like 4-ethyl pyridine gave 30% conversion with complete selectivity towards 1-(pyridin-4-yl) ethan-1-one. Most importantly, cyclic unsaturated compounds were also oxidized under the optimized conditions with excellent selectivity towards the corresponding product. The oxidation of α -pinene gave a 91.8% conversion with 100% verbenone selectivity, while 85% of cyclohexene was converted, giving 72% cyclohex-2-en-1-one, as the major product (Table 3, entries 7 and 8).

The catalyst was also examined for the oxidation of various aromatic amines. Benzyl amine was completely converted to 85% benzamide and 15% benzaldehyde (Table 4, entry 1). Also, we extended the substrate scope by selecting various aromatic amines. The electron-donating substrate, like 4-methoxy benzy-

lamine completely converted to give 4-methoxy benzamide with 75% selectivity (Table 4, entry 2). Further, the conversion in the case of 4-nitro benzylamine decreased to 60% with 40% selectivity (Table 4, entry 3). The catalyst was also efficient in converting difficult substrate like *N*-benzylpyridine-2-amine completely. However, the selectivity towards *N*-(pyridine-2-yl) benzamide was only 35.5% (Table 4, entry 4). In the case of dibenzyl amine, the presence of two active methylene groups gave 35% *N*-benzylbenzamide and the remaining side products like 26% benzaldehyde, 3.4% benzoic acid, 18.6% Benzenemethanamine, *N*-(phenylmethylene), and 17% Benzamide (Table 4, entry 5).

The oxidation of benzyl alcohol gave 70% benzaldehyde and 30% benzoic acid using the synthesized catalyst (Table 5, entry 1). Further, when the electron-donating substrate was used, the rate of reaction decreased with improved selectivity to aldehyde (Table 5, entry 2). The oxidation of 2-nitro benzyl alcohol gave 86% conversion with 50% selectivity, while 3-nitro benzyl alcohol gave 86% conversion and 68% selectivity. The oxidation of the benzyl alcohol with electron-withdrawing substituents like 4-chloro benzyl alcohol gave 90% conversion. However, the selectivity was very poor (Table 5, entry 5). Also, cyclic alcohols like cyclohexanol, cycloheptanol, and cyclooctanol were completely oxidized to the corresponding ketones in 16 h using 2 wt% $CuZrO_2$ (Table 5, entries 7–9).

3.2. Activity and mechanism

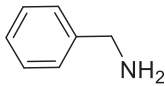
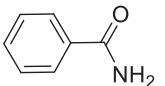
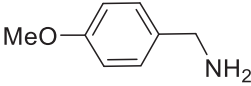
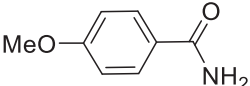
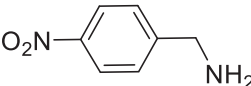
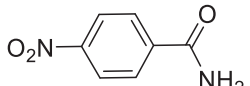
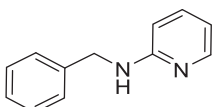
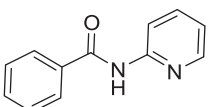
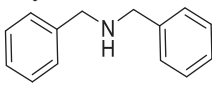
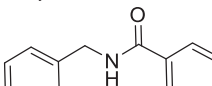
The EPR study of the solid catalyst has been reported to be a very effective technology to identify paramagnetic species in solid materials even when present in very low amounts and for the effective measurement of the surface oxygen vacancies [19]. Herein, we have performed solid EPR experiments at a different temperature ranging from -140 to 25 °C. EPR was applied to probe

Table 3
Results of oxidation of different ethylbenzene and cyclic alkenes with 2 wt% $CuZrO_2$ catalyst.^a

Entry	Substrate	Product	% Conv.	% Sel.
1.			98	100
2.			100	100
3.			98	100
4.			66	100
5.			60	80
6.			30	100
7.			91	100
8.			85	72

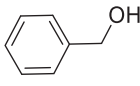
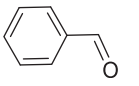
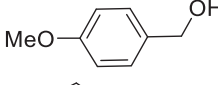
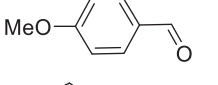
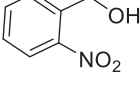
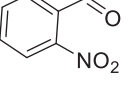
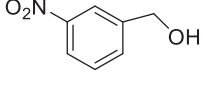
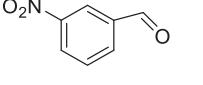
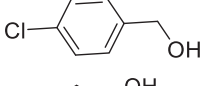
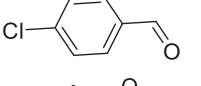
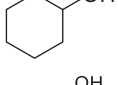
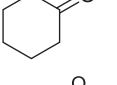
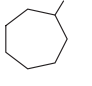
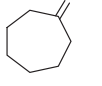
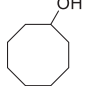
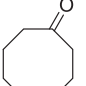
^a **Reaction conditions** Substrate: 1 mmol; Oxidant: aq. TBHP 3 mmol; 2 wt% $CuZrO_2$ catalyst: 15 mg.; Acetonitrile: 2 mL; Temp. 80 °C; Internal standard: Chlorobenzene 1 mmol; Reaction time: 18 h.

Table 4
Results of oxidation of different amines 2 wt% CuZrO₂ catalyst.^a

Entry	Substrate	Product	% Conv.	% Sel.
1.			100	85
2.			100	75
3.			60	40
4.			100	35
5.			100	35

^a **Reaction conditions** Substrate: 1 mmol; Oxidant: aq. TBHP 3 mmol; catalyst: 15 mg, 2 wt% CuZrO₂; Acetonitrile: 2 mL; Temp. 60 °C; Internal standard: Chlorobenzene 1 mmol; Reaction time: 9 h.

Table 5
Results of oxidation of different alcohols 2 wt% CuZrO₂ catalyst.^a

Entry	Substrate	Product	%Conv.	% Sel.
1 ^a			100	70
2 ^a			43	90
3 ^b			86	50
4 ^b			86	68
5 ^b			90	44
7 ^c			100	97
8 ^c			100	96
9 ^c			100	86

^a **Reaction conditions** Substrate: 1 mmol; Oxidant: aq. TBHP 3 mmol; 15 mg, catalyst: CuZrO₂; Reaction temp.: 60 °C; Acetonitrile: 2 mL; Internal Standard Chlorobenzene: 1 mmol; Reaction time: a. 7 h, b.9 h, c.16 h.

the hyperfine structure of the Cu species and the crystal structure of the 2 wt% CuZrO₂ catalyst. The signal centered around $g_{\perp} = 2.16$ and a magnetic field of 315 mT shows Cu²⁺ ions in the synthesized crystal catalyst. The feature of this $g_{\perp} = 2.16$ value and the magnetic field signal is mainly attributed to the dipolar broadening effect, which arises from the interaction between the paramagnetic

Cu²⁺ ion in the 2 wt% CuZrO₂ crystal system [32]. When decreasing the temperature from 25 to -140 °C, the peak intensity increased with no parallel peak signal of Cu in this system, which may be due to the lower percentage of Cu content in this catalyst system. This confirms the presence of Cu²⁺ species working as a radical initiator (Fig. 4).

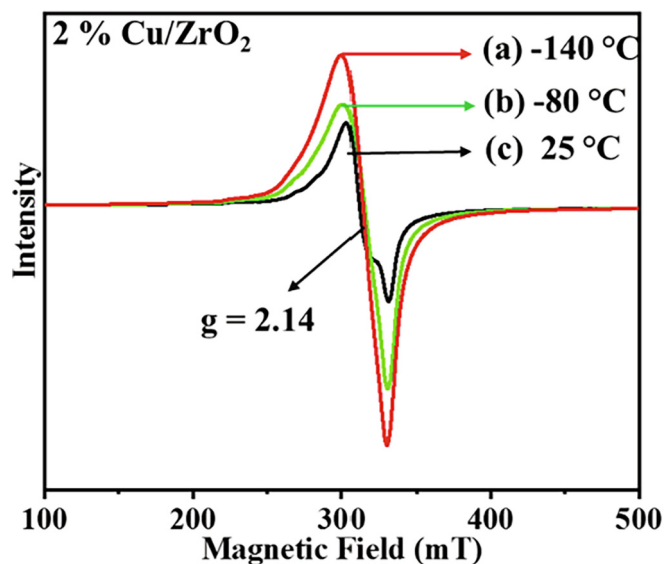
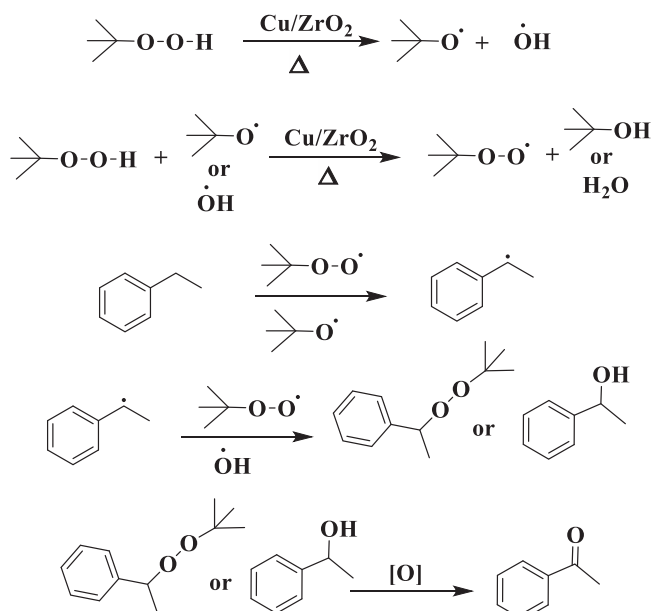


Fig. 4. Electron paramagnetic resonance (EPR) analysis of solid 2 wt% CuZrO₂ catalyst at different temperature (a) –140 °C, (b) –80 °C, and (c) 25 °C.

The mechanistic path for the Cu_xZrO_{100-x} catalyzed oxidation of ethylbenzene was confirmed using a free radical scavenger, hydroxyl butylated toluene (HBT). The reaction under the optimized conditions gave 98% selectivity with the complete formation of acetophenone (Scheme 3). However, in the presence of HBT, no forward reaction was observed, which confirmed that the reaction takes place via free radical formation. The proposed mechanism involves the adsorption of TBHP on the catalytic surface as the first step.

The reaction proceeds via a homolytic dissociation of TBHP giving activated radicals, which is considered to be the chain initiation step [33]. The *tert*-butoxy radical traps the benzylic proton from the substrate and forms a benzylic radical. On the other hand, the hydroxyl radical reacts with a fresh TBHP to form activated



Scheme 3. A plausible mechanism of ethylbenzene to acetophenone using Cu_x-ZrO_{100-x} catalyst.

tert-butyl peroxide radical [34]. In the last step, i.e., the termination step of the reaction, an intermediate is formed using a *tert*-butyl peroxide radical and substrate. This intermediate then dissociates to give acetophenone and TBHP *t*-butanol as the final products. A similar mechanistic route for the oxidation of benzyl alcohol is also proposed (see SI, S12).

4. Conclusions

Herein, we successfully synthesized Cubic Cu_xZrO_{100-x} by coprecipitation, followed by the hydrothermal method, at a far lower temperature than that reported. The synthesized catalysts were well characterized and all spectroscopic techniques agreed with the formation of CuO loaded on cubic zirconia. These catalysts were found to be highly active and gave almost complete conversion of active methyl groups, amines and alcohols under mild reaction conditions. It was also found that even at a low loading of Cu (i.e. 2 wt%) the catalyst was highly active. We believe that the cubic phase of the Cu_xZrO_{100-x} catalyst is responsible for the excellent oxidation activity. The reaction proceeded via the radical pathway giving different carbonyl groups and the catalyst was found to be highly recyclable.

Credit Author Statement

BDB performed the investigation, methodology, data curation, formal analysis, and wrote the original draft of the manuscript, JHA performed the formal analysis, wrote the original manuscript draft and performed the final review and editing of the manuscript. AVB conceptualized the idea, performed validation, writing the manuscript and supervision, and performed the final review and editing of the manuscript.

Declaration of Competing Interest

The authors declare that they have no known competing financial interests or personal relationships that could have appeared to influence the work reported in this paper.

Acknowledgements

CSMCRI communication No. 87/2020. BDB acknowledges the UGC government of India for a senior research fellowship. AVB acknowledges MLP-0028 for financial support. AESDCIF is highly acknowledged for all the requisite instrumental analysis.

Appendix A. Supplementary data

Supplementary data to this article can be found online at <https://doi.org/10.1016/j.poly.2021.115129>.

References

- [1] M.B. Gawande, R.K. Pandey, R.V. Jayaram, Role of mixed metal oxides in catalysis science – versatile applications in organic synthesis, *Catal. Sci. Tech.* 2 (2012) 1113–1125.
- [2] I.E. Wachs, K. Routray, *Catalysis science of bulk mixed oxides*, *ACS Catal.* 2 (6) (2012) 1235–1246.
- [3] I.E. Wachs, J.-M. Jehng, W. Ueda, Determination of the chemical nature of active surface sites present on bulk mixed metal oxide catalysts †, *J. Phys. Chem. B* 109 (6) (2005) 2275–2284.
- [4] K. Tanabe, M. Misono, Y. Ono, H. Hattori, *New Solid Acids and Bases: Their Catalytic Properties*, Elsevier, Amsterdam, *Studies in Surface Science and Catalysis*, 1989, 51.
- [5] M. Konsolakis, *The role of Copper–Ceria interactions in catalysis science: Recent theoretical and experimental advances*, *Appl. Catal. B: Environ.* 198 (2016) 49–66.
- [6] P.P. Singh, T. Thatikonda, K.A.A. Kumar, S.D. Sawant, B. Singh, A.K. Sharma, P.R. Sharma, D. Singh, R.A. Vishwakarma, Cu–Mn spinel oxide catalyzed

- regioselective halogenation of phenols and N-heteroarenes, *J. Org. Chem.* 77 (13) (2012) 5823–5828.
- [7] R. Xie, G. Fan, L. Yang, F. Li, Hierarchical flower-like Co–Cu mixed metal oxide microspheres as highly efficient catalysts for selective oxidation of ethylbenzene, *Chem. Eng. J.* 15 (2016) 288 169–78.
- [8] A. Shukla, R.K. Singha, L.N.S. Konathala, T. Sasaki, R. Bal, Catalytic oxidation of aromatic amines to azoxy compounds over a Cu–CeO₂ catalyst using H₂O₂ as an oxidant, *RSC Adv.* 6 (27) (2016) 22812–22820.
- [9] S. Sadjadi, V. Farzaneh, S. Shirvani, M. Ghashghae, Preparation of Cu–MgO catalysts with different copper precursors and precipitating agents for the vapor-phase hydrogenation of furfural, *Korean J. Chem. Eng.* 34 (3) (2017) 692–700.
- [10] L. Petitjean, R. Gagne, E.S. Beach, D. Xiao, P.T. Anastas, Highly selective hydrogenation and hydrogenolysis using a copper-doped porous metal oxide catalyst, *Green Chem.* 18 (1) (2016) 150–156, <https://doi.org/10.1039/C5GC01464F>.
- [11] K. Samson, M. Sliwa, R.P. Socha, K. Góra-Marek, D. Mucha, D. Rutkowska-Zbik, J.F. Paul, M. Ruggiero-Mikoajczyk, R. Grabowski, J. Soczyński, Influence of ZrO₂ structure and copper electronic state on activity of Cu/ZrO₂ catalysts in methanol synthesis from CO₂, *ACS Catal.* 4 (2014) 3730–3741.
- [12] S. Tada, S. Kayamori, T. Honma, H. Kamei, A. Nariyuki, K. Kon, T. Toyao, K.I. Shimizu, S. Satokawa, Design of Interfacial Sites between Cu and Amorphous ZrO₂ Dedicated to CO₂-to-Methanol Hydrogenation, *ACS Catal.* 8 (2018) 7809–7819.
- [13] E. Lam, K. Larmier, P. Wolf, S. Tada, O.V. Safonova, C. Copéret, Isolated Zr Surface Sites on Silica Promote Hydrogenation of CO₂ to CH₃OH in Supported Cu Catalysts, *JACS.* 140 (2018) 10530–10535.
- [14] C. Zhong, X. Guo, D. Mao, S. Wang, G. Wu, G. Lu, Effects of alkaline-earth oxides on the performance of a CuO–ZrO₂ catalyst for methanol synthesis via CO₂ hydrogenation, *RSC Adv.* 5 (2015) 52958–52965.
- [15] P. Chandra, D.S. Doke, S.B. Umbarkar, A.V. Biradar, One-pot synthesis of ultrasmall MoO₃ nanoparticles supported on SiO₂, TiO₂, and ZrO₂ nanospheres: An efficient epoxidation catalyst, *J. Mater. Chem. A* 2 (2014) 19060–19066.
- [16] V.R. Acham, A.V. Biradar, M.K. Dongare, E. Kemnitz, S.B. Umbarkar, Palladium nanoparticles supported on magnesium hydroxide fluorides: A selective catalyst for olefin hydrogenation, *ChemCatChem.* 6 (2014) 3182–3191.
- [17] R.H. Nielsen, J.H. Schlewitz, H. Nielsen, & Updated by Staff, Zirconium and zirconium compounds, *Kirk-Othmer Encyclopedia of Chemical Technology* (2000) 1–46.
- [18] B.Q. Xu, T. Yamaguchi, K. Tanabe, Acid-base bifunctional behavior of ZrC₂ in dual adsorption of CO₂ and NH₃, *Chem. Lett.* 17 (10) (1988) 1663–1666.
- [19] M.K. Dongare, V. Ramaswamy, C.S. Gopinath, A.V. Ramaswamy, S. Scheurell, M. Brueckner, E. Kemnitz, Oxidation activity and ¹⁸O-isotope exchange behavior of Cu-stabilized cubic zirconia, *J. Catal.* 199 (2) (2001) 209–216.
- [20] J.S. Valente, M. Valle-Orta, H.A. Herrera, R.Q. Solórzano, P. Angel, J.R. Salgado, J. R. Montiel-López, Controlling the redox properties of nickel in NiO/ZrO₂ catalysts synthesized by sol–gel, *Catal. Sci. Tech.* 8 (16) (2018) 4070–4082.
- [21] H. Hayashi, Y. Hakuta, Hydrothermal Synthesis of metal oxide nanoparticles in supercritical water, *Materials* 3 (2010) 3794–3817.
- [22] M.K. Dongare, K. Malshe, C.S. Gopinath, I.K. Murwani, E. Kemnitz, Oxidation activity and ¹⁸O-isotope exchange behavior of nickel oxide-stabilized cubic zirconia, *J. Catal.* 222 (2004) 80–86.
- [23] Y.-P. Sun, T. Adschiri, K. Arai, Hydrothermal synthesis of metal oxide nanoparticles under supercritical conditions, supercritical fluid technology, *Mater. Sci. Eng.* (2002) 227–235.
- [24] V. Ramaswamy, M. Bhagwat, D. Srinivas, A.V. Ramaswamy, Structural and spectral features of nano-crystalline copper-stabilized zirconia, *Catal. Today* 97 (2004) 63–70.
- [25] A. Sinhamahapatra, J.P. Jeon, J. Kang, B. Han, J.S. Yu, Oxygen-deficient zirconia (ZrO_{2-x}): a new material for solar light absorption, *Sci. Rep.* 6 (1) (2016) 1–8.
- [26] J. Yu, J. Kiwi, T. Wang, C. Pulgarin, S. Rtimi, Duality in the mechanism of hexagonal zno/cuxo nanowires inducing sulfamethazine degradation under solar or visible light, *Catalysts* 9 (2019) 916.
- [27] G. Ananya, N. Pranati, S. Ramaprabhu, Investigation of the role of Cu₂O beads over the wrinkled graphene as an anode material for lithium ion battery, *Int. J. Hydrog. Energy* 41 (2016) 3974–3980.
- [28] G.A. Burdock, Fenaroli's Handbook of Flavor Ingredients, CRC Press, 2016.
- [29] M. Sittig, *Pharmaceutical manufacturing encyclopedia*. Noyes Publications, (1988).
- [30] A. Ojeda-Porras, D. Gamba-Sánchez, Recent developments in amide synthesis using nonactivated starting materials, *J. Org. Chem.* 81 (2016) 11548–11555.
- [31] V. R. Choudhary, B. S. Uphade, S. G. Pataskar, and A. Keshavaraja, *Angew. Chem.* (1996), 35, 2393–2394.
- [32] J. Wang, T. Yu, X. Wang, G. Qi, J. Xue, M. Shen, W. Li, The influence of silicon on the catalytic properties of Cu/SAPO-34 for NO_x reduction by ammonia-SCR, *Appl. Catal. B: Env.* 127 (2012) 137–147.
- [33] J. Tan, T. Zheng, Y. Yu, K. Xu, TBHP-promoted direct oxidation reaction of benzylic C sp³–H bonds to ketones, *RSC adv.* 7 25 (2017) 15176–80.
- [34] T. Liu, H. Cheng, L. Sun, F. Liang, C. Zhang, Z. Ying, W. Lin, F. Zhao, Synthesis of acetophenone from aerobic catalytic oxidation of ethylbenzene over Ti–Zr–Co alloy catalyst: Influence of annealing conditions, *Appl. Catal. A-Gen.* 25 (512) (2016) 9–14.